Applied Physics Letters

Motion of skyrmioniums with negligible deformation in synthetic antiferromagnets

Cite as: Appl. Phys. Lett. **121**, 012403 (2022); https://doi.org/10.1063/5.0095984
Submitted: 14 April 2022 • Accepted: 20 June 2022 • Published Online: 05 July 2022

Ziyang Yu, Bin Gong, Chenhuinan Wei, et al.

AIP Publishing

Applied Physics Letters ARTICLE scitation.org/journal/apl

Motion of skyrmioniums with negligible deformation in synthetic antiferromagnets

Cite as: Appl. Phys. Lett. **121**, 012403 (2022); doi: 10.1063/5.0095984
Submitted: 14 April 2022 · Accepted: 20 June 2022 ·
Published Online: 5 July 2022

Ziyang Yu,[1] Bin Gong,[1] Chenhuinan Wei,[2] Rui Wang,[1] Lun Xiong,[1,a)] Long You,[3] Yue Zhang,[3,a)] Shiheng Liang,[4] Zhihong Lu,[5] and Rui Xiong[6]

AFFILIATIONS

[1]Hubei Key Laboratory of Optical Information and Pattern Recognition, School of Optical Information and Energy Engineering, Wuhan Institute of Technology, Wuhan 430205, People's Republic of China
[2]Hubei Provincial Key Laboratory of Green Materials for Light Industry, Hubei University of Technology, Wuhan 430068, China
[3]School of Optical and Electronic Information, Huazhong University of Science and Technology, Wuhan 430074, China
[4]Faculty of Physics and Electronic Science, Hubei University, Wuhan 430062, China
[5]The State Key Laboratory of Refractories and Metallurgy, School of Materials and Metallurgy, Wuhan University of Science and Technology, Wuhan 430081, China
[6]Key Laboratory of Artificial Micro- and Nano-Structures of Ministry of Education, School of Physics and Technology, Wuhan University, Wuhan 430072, China

[a)]**Authors to whom correspondence should be addressed:** xionglun@wit.edu.cn and yue-zhang@mail.hust.edu.cn

ABSTRACT

A skyrmionium is a magnetic texture composed of two skyrmions with opposite winding numbers (Q) and different sizes. Compared to a skyrmion, a skyrmionium can move at a higher velocity. However, a moving skyrmionium may still deform because of the local skyrmion Hall effect resulting from the two skyrmions with opposite Q. In this study, we propose a skyrmionium motion with negligible deformation in a synthetic antiferromagnetic (AFM) medium, composed of a free ferromagnetic (FM) layer with a skyrmionium and a pinned FM layer with uniform magnetization. The suppression of the skyrmionium deformation is due to the enhanced coupling between the inner and outer skyrmion under interlayer AFM coupling. This study paves the way for the development of devices with high stability, high processing speed, and small sizes.

A skyrmion is a circular magnetic texture with nontrivial topological properties and small size (10–100 nm).[1] Skyrmions exhibit potential applications in the field of information techniques and have been widely investigated in recent years.[2–8] However, several challenges remain for skyrmion-based devices. A typical example is the skyrmion Hall effect (SkHE), which originates from the nonzero topological charge of a skyrmion. This SkHE gives rise to a transversal velocity for a skyrmion moving along a nanowire,[6,9–11] which in turn increases the risk of annihilation.[9,11–13]

To depress SkHEs, many efforts have been made to fabricate a composite composed of two skyrmions with opposite topological numbers. In addition to coupled skyrmions with opposite winding numbers (Q, $+1$, or -1) and same size in a synthetic antiferromagnetic (SAF) structure,[14] a skyrmionium is another composite of two skyrmions with opposite topological charges and different sizes.[13] Since it was first observed in 2013,[15] several studies have shown that a ferromagnetic (FM) skyrmionium can be created by a spin-polarized current,[10] magnetic field pulses,[16] or strain mediation.[17] Also, a skyrmionium can be induced to move under a spin-transfer torque (STT), spin–orbit torque (SOT), or spin wave.[18–26]

Given that the total topological charge of a skyrmionium is zero, one may expect the absence of SkHE. However, local SkHE for two skyrmions with opposite Q still matters, because it can lead to transversal motion of both skyrmions in opposite directions. This can deform and even disintegrate a skyrmionium under a strong driving force. Therefore, stabilizing the moving skyrmionium remains a critical problem. It is noteworthy that both skyrmions in a skyrmionium are not independent, and there is magnetostatic and exchange coupling between them, which plays an important role in controlling the deformation of a skyrmionium. Therefore, manipulation of the interactions between both skyrmions may be a key for stabilizing a skyrmionium.

In this Letter, we report our numerical investigation on skyrmionium motion driven by STT and SOT in an SAF nanostructure with Ruderman–Kittel–Kasuya–Yosida (RKKY) AFM exchange coupling between both FM layers. A skyrmionium is generated in the free layer with low anisotropy energy, whereas the magnetization in the pinned layer with high anisotropy energy is spatially homogenous. The skyrmionium is driven by STT or SOT under an injected current [Fig. 1(a)]. We show that the skyrmionium can move along the middle line of the nanotrack without distortion under moderate RKKY exchange coupling. The suppressed deformation is attributed to enhanced exchange coupling between the two skyrmions under RKKY coupling. This study paves the way for the design of future skyrmionic applications with improved stability, high reading speed, and small sizes.

We consider an SAF multilayer composed of a free FM layer, a pinned FM layer, and a nonmagnetic layer which is the medium for RKKY coupling. We first studied the stability of a skyrmionium in an SAF nanodisk and then investigated the skyrmionium motion in an SAF nanotrack. The radius (R) of the nanodisk was 200 nm, whereas the thicknesses of the FM and nonmagnetic layers were all 0.4 nm with a cell dimension of $1 \times 1 \times 0.4\,\mathrm{nm}^3$. The size of the nanotrack was as follows: The length and width of the nanotrack were 1100 and 200 nm, respectively. Both FM layers had the same thickness (0.4 nm), and the distance between them was 0.4 nm along with a cell size of $2 \times 2 \times 0.4\,\mathrm{nm}^3$.

Skyrmionium motion was simulated using object-oriented micromagnetic framework (OOMMF) software containing a code of interfacial Dzyaloshinskii–Moriya interaction (DMI).[27] The simulation was based on numerically solving the Landau–Lifshitz–Gilbert (LLG) equation containing both STT and SOT terms[28,29]

$$\frac{\partial \vec{m}}{\partial t} = -\gamma_0 \vec{m} \times \vec{H}_{eff} + \alpha\left(\vec{m} \times \frac{\partial \vec{m}}{\partial t}\right) + \underbrace{\frac{u\vec{m} \times \left(\vec{m} \times \frac{\partial \vec{m}}{\partial x}\right) + \beta u \vec{m} \times \frac{\partial \vec{m}}{\partial x}}{STT\ term}}_{} + \underbrace{\frac{\gamma H_{SO} \vec{m} \times (\vec{\sigma} \times \vec{m})}{SOT\ term}}_{}. \quad (1)$$

Here, $\vec{m}$, t, and γ are the unit magnetization vector, time, and gyromagnetic ratio of the electrons, respectively. The first and second terms on the right-hand side of Eq. (1) contribute to the torque from the effective magnetic field $\vec{H}_{eff}$ and Gilbert damping, respectively. The third and fourth terms depict adiabatic and non-adiabatic STTs, respectively. The velocity of the electron u can be estimated using $u = \frac{JPg\mu_B}{2eM_s}$, where J is the current density, P is the polarization rate, g is the Landé factor, μ_B is the Bohr magneton, and e is the electron charge. H_{so} is the SOT effective field: $H_{so} = \frac{\mu_B \theta_{SH} J}{\gamma_0 e M_s a}$, where θ_{SH} is the spin Hall angle and a is the thickness of the free FM layer. The parameter γ_0 is related to γ by $\gamma_0 = \mu_0|\gamma|$.

We exploited the parameters of a Pt/Co system with perpendicular magnetic anisotropy.[4,30–33] The saturation magnetization (M_S) and exchange stiffness constant (A) were 5.8×10^5 A/m and 1.5×10^{-11} J/m, respectively. The DMI constant (D) was 1 and 4 mJ/m^2. The anisotropy constant for the lower pinned FM layer (K_{low}) was 5×10^6 J/m^3, and that of the upper free layer (K_{up}) varied between 1×10^5 and 6×10^5 J/m^3. $P = 0.7$. The damping coefficient was α=0.2, and the coefficient of the non-adiabatic STT was β=0.4.

First, we considered the stability of a skyrmionium in an SAF nanodisk. Without interlayer RKKY coupling, the skyrmionium could be stabilized within 2 ns. The inner and outer diameters were 90 and 150 nm, respectively [Fig. 2(a)]. Under interlayer RKKY exchange coupling with $J_{ex} = -5 \times 10^{-5}$ J/m^2, the inner and outer diameters were reduced to 19 and 34 nm, respectively [Fig. 2(b)].

Stabilization of a skyrmionium results from a trade-off among different free energies. Figures 2(c) and 2(d) show the evolution of free energies during relaxation. In the absence of RKKY coupling, the demagnetization energy (E_{dem}), exchange energy (E_{exc}), and DMI energy (E_{dmi}) decreased and approached constant values quickly, while the uniaxial perpendicular anisotropy energy (E_{anis}) increased. In contrast, under RKKY coupling, the decrease in the RKKY AFM exchange energy (E_{RKKY}) mainly contributed to the stabilization of the skyrmionium. In principle, the lowest E_{RKKY} corresponds to perfect antiparallel alignment of the magnetization in both FM layers. This annihilates a skyrmionium. However, E_{exc} between the inner and outer skyrmions increases when they approach each other, and this energy barrier of E_{exc} suppresses the deformation and annihilation of the skyrmionium. Therefore, a stable small skyrmionium can still be formed under competition between E_{RKKY} and E_{exc}.

We simulated the skyrmionium motion driven by the STT and SOT in an SAF nanotrack as shown in Fig. 1 [Figs. 3(a) and 3(d)]. For comparison, we also studied the STT and SOT-induced skyrmionium motion in a single FM layer [Figs. 3(b) and 3(e)] and the skyrmion motion driven by STT and SOT in an SAF nanotrack [Figs. 3(c) and 3(f)]. At $J_{ex} = -5 \times 10^{-6}$ J/m^2, under both STT and SOT, the skyrmionium was able to move strictly along the middle line of the SAF track with negligible deformation [Figs. 3(a) and 3(d)]. In comparison,

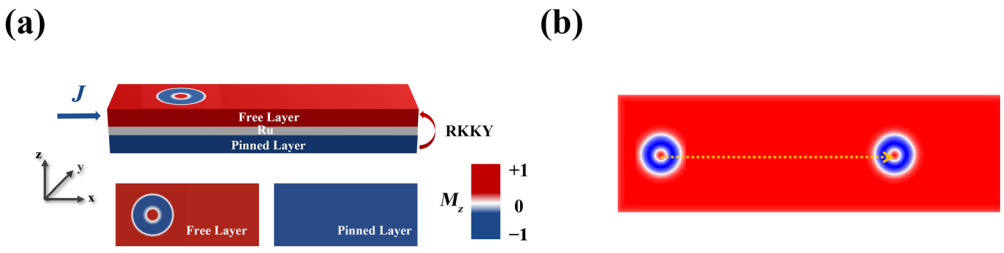

FIG. 1. (a) Schematic of an SAF nanowire composed of a free FM layer with a small magnetic anisotropy constant and a pinned FM layer with a large one. (The skyrmionium exists in the upper free FM layer, and its motion is induced by the STT effect under an injected current.) (b) Motion of a skyrmionium with negligible dislocation in the SAF nanowire shown in (a).

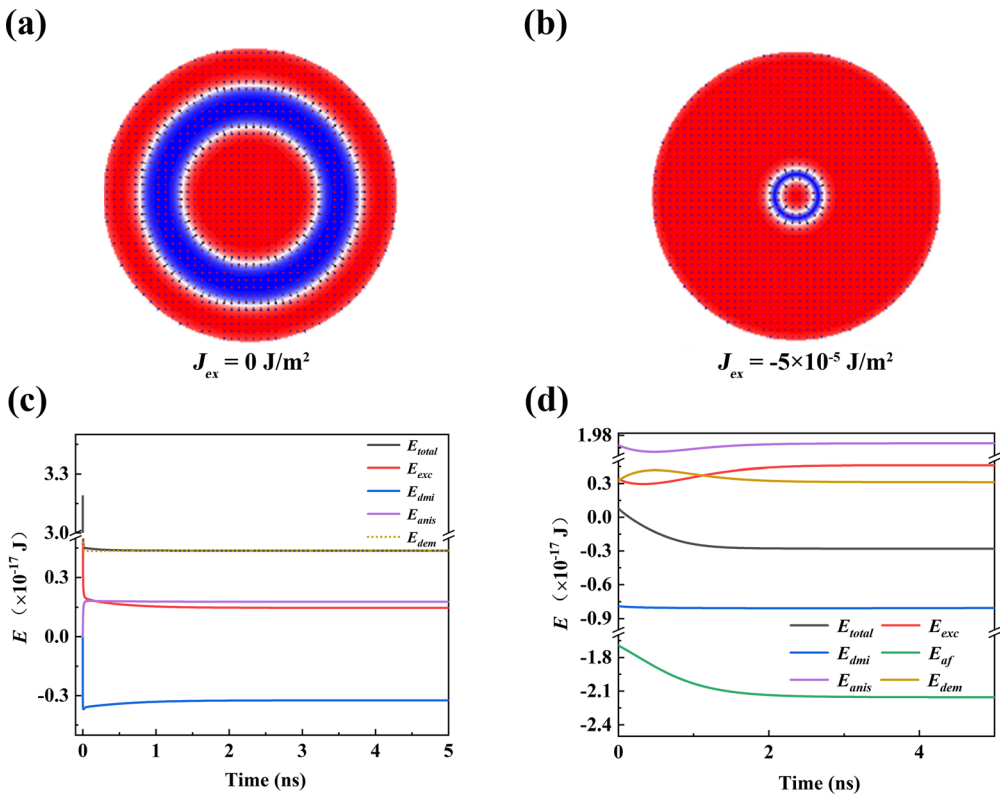

FIG. 2. Profile of a stable skyrmionium with (a) $J_{ex} = 0$ J/m^2 and (b) $J_{ex} = -5 \times 10^{-5}$ J/m^2; (c) evolution of magnetic free energies for a skyrmionium with (c) and without (d) antiferromagnetic exchange interaction ($J_{ex} = -5 \times 10^{-5}$ J/m^2 or 0 J/m^2, $D = 3$ mJ/m^2, $K_{up} = 4 \times 10^5$ J/m^2, and $K_{low} = 3 \times 10^6$ J/m^2).

in the absence of RKKY exchange coupling, the skyrmionium significantly dislocated due to the transversal deviation of the inner and outer skyrmions toward opposite directions [Figs. 3(b) and 3(e)]. Concerning the skyrmion driven by the STT and SOT in the SAF track with $J_{ex} = -5 \times 10^{-6}$ J/m^2, the skyrmion deviated toward the track edge owing to the SkHE [Figs. 3(c) and 3(f)].

Skyrmionium deformation is influenced by the interaction between the two skyrmions forming the skyrmionium. As shown in Fig. 2, under interlayer RKKY exchange coupling, the contraction of the skyrmionium can enhance this interaction between both skyrmions, which suppresses the dislocation of the skyrmionium.

Based on the results in Fig. 3, we conclude that RKKY exchange coupling contributes to the stability of a skyrmionium driven by both STT and SOT. We further studied the manipulation of the longitudinal velocity (v_x) of the skyrmionium. Note that v_x is proportional to J under both STT and SOT, and RKKY coupling clearly improves the stability of the skyrmionium [Figs. 4(a) and 4(b)]. Without RKKY coupling, deformation occurred under small current density ($J = 5 \times 10^{12}$ A/m^2 for STT and $J = 3 \times 10^9$ A/m^2 for SOT). However, under moderate RKKY coupling with $J_{ex} = 5 \times 10^{-6}$ J/m^2, the deformation was significantly suppressed. Regarding STT, the skyrmionium kept stable when J was as high as 10^{13} A/m^2. For SOT, the skyrmionium deformed and broke down when J was greater than 3×10^{10} and 5×10^{10} A/m^2, respectively. Both are significantly higher values than those without RKKY coupling.

Figures 4(c) and 4(d) show the variation in v_x as a function of J_{ex} at $J = 8 \times 10^{12}$ A/m^2 for STT and $J = 5 \times 10^9$ A/m^2 for SOT. The skyrmionium slowly moved under weak RKKY coupling due to deformation, and v_x reached its maximum value when J_{ex} was -1×10^{-6} J/m^2. Under stronger RKKY coupling, the change in v_x for STT was very small, whereas v_x for SOT clearly decreased. This indicates that moderate RKKY exchange coupling plays a key role in stabilizing the skyrmionium driven by either STT or SOT, which allows the skyrmionium to move at high velocities.

In theory, the motion of a rigid magnetic texture driven by STT and SOT can be analyzed by Thiele equations[34]

$$\vec{G} \times \vec{v}^{SOT} - \alpha \mathcal{D} \cdot \vec{v}^{SOT} + 4\pi \boldsymbol{B} \cdot \vec{j} + \vec{F} = 0, \tag{2}$$

$$\vec{G} \times (\vec{v}^{STT} - \vec{u}) + \mathcal{D} \cdot (\beta \vec{u} - \alpha \vec{v}^{STT}) + \vec{F} = 0. \tag{3}$$

In Eqs. (2) and (3), $\vec{G} = (0, 0, 4\pi Q)$ is the gyromagnetic factor, $\vec{v}^{SOT(STT)} = \left(v_x^{SOT(STT)}, v_y^{SOT(STT)}\right)$ is the texture velocity, and $\vec{j} = (j, 0)$ is the driving current density. $\mathcal{D} = 4\pi \begin{pmatrix} \mathcal{D}_{xx} & \mathcal{D}_{xy} \\ \mathcal{D}_{yx} & \mathcal{D}_{yy} \end{pmatrix}$ is the dissipative force tensor with components $\mathcal{D}_{ij} = \frac{1}{4\pi} \int \frac{\partial \boldsymbol{m}}{\partial i} \cdot \frac{\partial \boldsymbol{m}}{\partial j} dxdy$. $\boldsymbol{B} = \frac{u}{aJ} \begin{pmatrix} -I_{xy} & I_{xx} \\ -I_{yy} & I_{yx} \end{pmatrix}$ is the driving force tensor of SOT with the

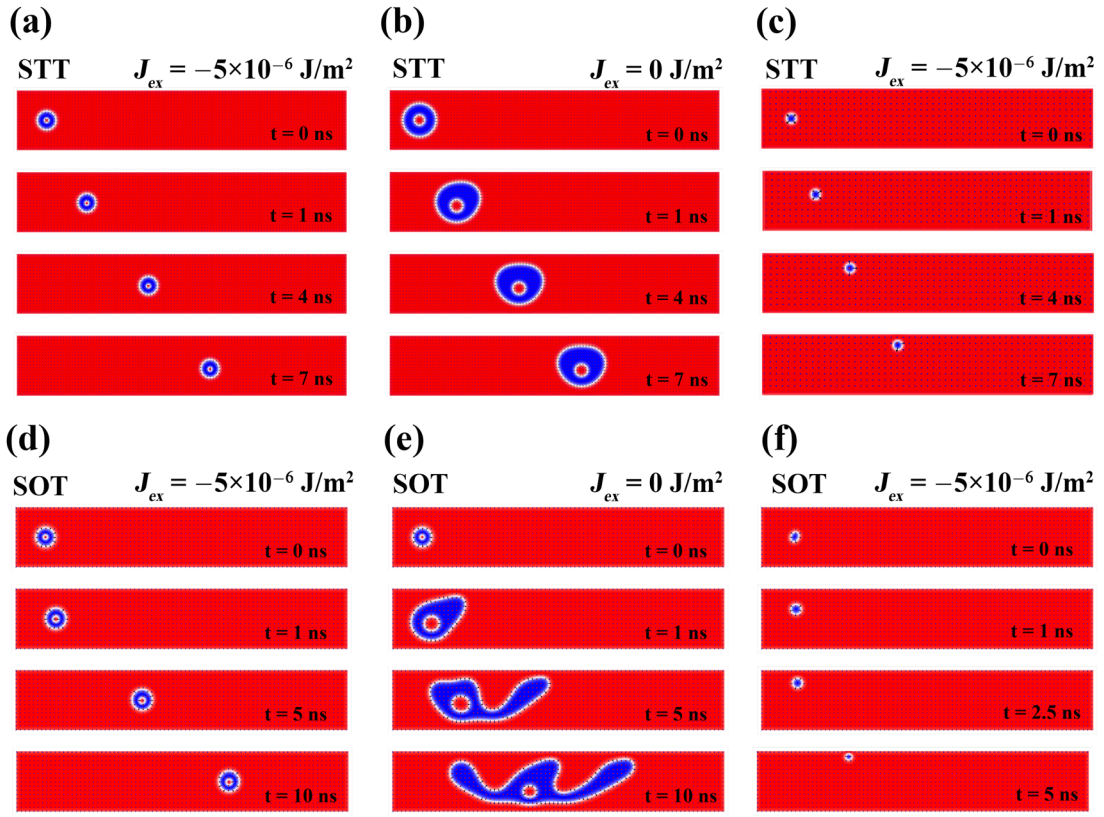

FIG. 3. Snapshots of skyrmionium motion driven by (a) STT and (d) SOT with $J_{ex} = -5 \times 10^{-6}$ J/m^2. Snapshots of skyrmionium motion driven by (b) STT and (e) SOT with $J_{ex} = 0$ J/m^2. Snapshots of skyrmion motion triggered by (c) STT and (f) SOT with $J_{ex} = -5 \times 10^{-6}$ J/m^2. ($D = 3.5$ mJ/m^2, $K_{up} = 5 \times 10^5$ J/m^2, $K_{low} = 5 \times 10^6$ J/m^2. Current densities of STT and SOT: $J_{STT} = 8 \times 10^{12}$ A/m^2 and $J_{SOT} = 5 \times 10^9$ A/m^2).

components $I_{ij} = \frac{1}{4\pi}\int \left(\frac{\partial \boldsymbol{m}}{\partial i} \times \boldsymbol{m}\right)_j dxdy$, a is 0.4×10^{-9} m, the thickness. $\vec{F}$ stands for the force from the edge of the nanowire.

Because of the trivial topological properties of the skyrmionium, the first terms in Eqs. (2) and (3) can be ignored. In addition, owing to the absence of SkHE, the skyrmionium moves strictly along the middle line, and the total boundary force acting on the skyrmionium is zero. Therefore, the boundary force terms in Eqs. (2) and (3) are ignored. Under these circumstances, v_x for steady motion can be derived as follows:

$$v_x^{SOT} = \frac{uI_{xy}}{a\alpha \mathcal{D}_{xx}} \tag{4}$$

and

$$v_x^{STT} = \frac{\beta u}{\alpha}. \tag{5}$$

Equations (4) and (5) reveal that the velocity of the skyrmionium driven by STT is related to the velocity of the propagating electrons and magnetic parameters α and β. Therefore, when the interlayer coupling is strong enough to suppress the deformation, the skyrmionium velocity reaches a stable value. Further reduction in the skyrmionium size under stronger RKKY coupling does not influence the velocity [Fig. 4(c)]. However, under SOT, the skyrmionium velocity also depends on I_{xy} and D_{xx}, which are related to the magnetization structure of the skyrmionium. The reduction in the skyrmionium size under strong RKKY coupling results in a decrease in I_{xy} and D_{xx} [the inset of Fig. 4(d)]. However, the decrease in I_{xy} is dominant over that of D_{xx}, which leads to decreased I_{xy}/D_{xx} and skyrmionium velocity. Based on Eqs. (4) and (5), we calculated the skyrmionium velocity when J_{ex} was larger than that for the maximum velocity. (The skyrmionium deformation under a smaller J_{ex} invalids Thiele equations.) The calculated results are close to that obtained by OOMMF simulation [Figs. 4(c) and 4(d)].

Finally, we briefly discuss potential applications of this study. Coupled skyrmion systems, such as skyrmionium and AFM coupled skyrmions in an SAF system, may contribute to the suppression of SkHE. However, a skyrmionium still deforms owing to the local SkHE, and in an SAF system, the cancelation of the magnetization in AFM-coupled skyrmions increases the difficulty for detecting skyrmions.[32,35] In this study, RKKY coupling between the skyrmionium and the pinned FM layer clearly improved the stability of skyrmionium. Nevertheless, the magnetization of the two layers was not canceled owing to the uniform magnetization in the pinned FM layer. Therefore, the proposed method provides a possible route for stabilizing a skyrmionium without sacrificing readability.

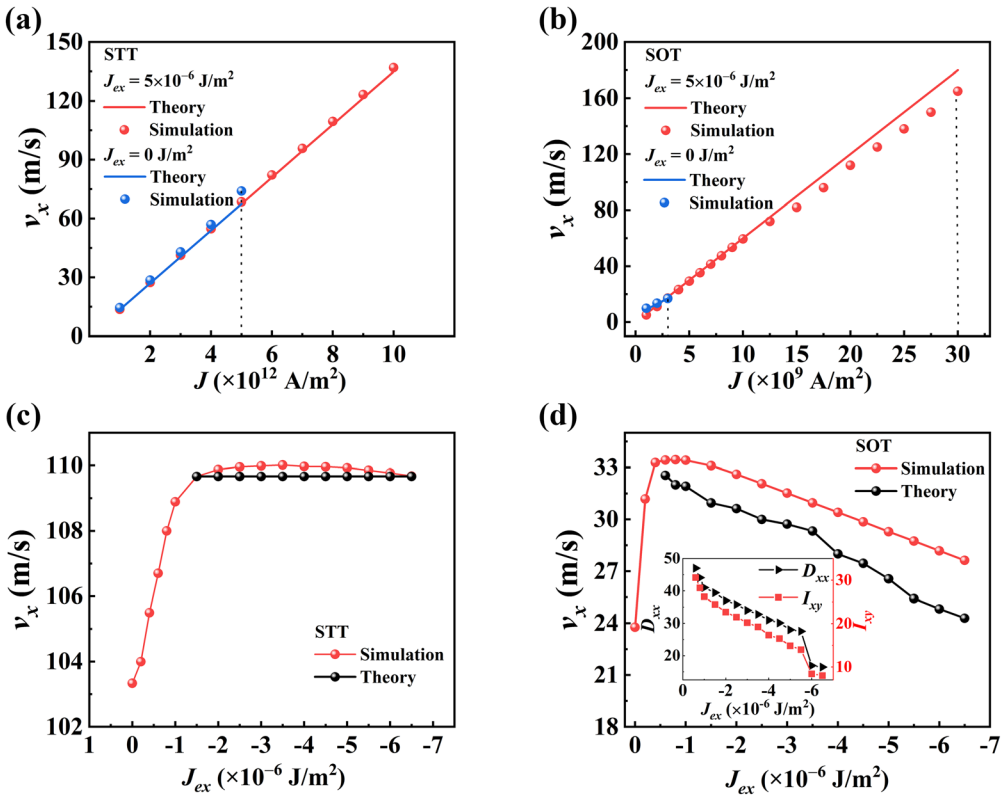

FIG. 4. v_x as a function of J for skyrmionium driven by (a) STT and (b) SOT at $J_{ex} = 5 \times 10^{-6}$ J/m^2 (red) and 0 J/m^2 (blue). [The dots and solid lines are the simulation and theoretical prediction based on Eqs. (4) and (5), respectively. Here, $D = 3.5$ mJ/m^2, $J_{ex} = -5 \times 10^{-6}$ J/m^2, $K_{up} = 5 \times 10^5$ J/m^2, and $K_{low} = 5 \times 10^6$ J/m^2.] v_x as a function of J_{ex} for skyrmionium driven by (c) STT ($J = 8 \times 10^{12}$ A/m^2) and (d) SOT ($J = 5 \times 10^9$ A/m^2). [The red and black dotted lines are the simulation and theoretical prediction based on Eqs. (4) and (5), respectively. Here, $D = 3.5$ mJ/m^2, $K_{up} = 5 \times 10^5$ J/m^2, and $K_{low} = 5 \times 10^6$ J/m^2. The inset in Fig. 4(d) shows the calculated values of I_{xy} and D_{xx} as a function of J_{ex} for skyrmionium motion under SOT.]

In summary, we investigated STT- and SOT-induced skyrmionium motion with negligible deformation in an SAF nanodisk under moderate RKKY AFM exchange coupling between the two FM layers. This absence of deformation results from the enhanced interaction between the two skyrmions comprising the skyrmionium under the RKKY coupling. Owing to this RKKY exchange coupling, the skyrmionium can move at high velocities (>150 m/s) with small size. These advantages pave the way for developing potential skyrmionium devices with high density, high processing speed, and good stability such as skyrmionium-based racetrack memory and artificial synaptic devices for neuromorphic computing.

The authors acknowledge financial support from the National Key Research and Development Program of China (No. 2022YFE0103300), the National Natural Science Foundation of China (Nos. 12104348, 51971098, and 11804211), the Major Research plan of the National Natural Science Foundation of China (No. 91963207), Science and Technology Department of Hubei Province (No. 2019CFB435), and the Graduate Innovative Fund of Wuhan Institute of Technology (Nos. CX2021376 and CX2021388).

AUTHOR DECLARATIONS

Conflict of Interest

The authors have no conflicts to disclose.

Author Contributions

Ziyang Yu: Conceptualization (equal); Data curation (equal); Formal analysis (equal); Funding acquisition (equal); Investigation (equal); Methodology (equal); Project administration (equal); Resources (equal); Writing – original draft (equal). **Bin Gong:** Data curation (equal); Formal analysis (equal); Software (equal); Writing – original draft (equal). **Chenhuinan Wei:** Resources (equal); Software (equal); Visualization (equal). **Rui Wang:** Visualization (equal). **Lun Xiong:** Formal analysis (equal); Supervision (equal); Validation (equal). **Long You:** Validation (equal). **Yue Zhang:** Conceptualization (equal); Formal analysis (equal); Supervision (equal); Writing – original draft (equal); Writing – review and editing (equal). **Shiheng Liang:** Visualization (equal). **Zhihong Lu:** Supervision (equal); Validation (equal); **Rui Xiong:** Supervision (equal); Validation (equal).

DATA AVAILABILITY

The data that support the findings of this study are available from the corresponding authors upon reasonable request.

REFERENCES

[1]A. G. Kolesnikov, M. E. Stebliy, A. S. Samardak, and A. V. Ognev, Sci. Rep. **8**(1), 16966 (2018).
[2]J. Tang, Y. D. Wu, W. W. Wang, L. Y. Kong, B. Y. Lv, W. S. Wei, J. D. Zang, M. L. Tian, and H. F. Du, Nat. Nanotechnol. **16**(10), 1086 (2021).
[3]K. Litzius, J. Leliaert, P. Bassirian, D. Rodrigues, S. Kromin, I. Lemesh, J. Zazvorka, K. J. Lee, J. Mulkers, N. Kerber, D. Heinze, N. Keil, R. M. Reeve, M. Weigand, B. Van Waeyenberge, G. Schuetz, K. Everschor-Sitte, G. S. D. Beach, and M. Klaui, Nat. Electron. **3**(1), 30 (2020).
[4]J. Sampaio, V. Cros, S. Rohart, A. Thiaville, and A. Fert, Nat. Nanotechnol. **8**(11), 839 (2013).
[5]W. Jiang, P. Upadhyaya, W. Zhang, G. Yu, M. B. Jungfleisch, F. Y. Fradin, J. E. Pearson, Y. Tserkovnyak, K. L. Wang, O. Heinonen, S. G. E. te Velthuis, and A. Hoffmann, Science **349**(6245), 283 (2015).
[6]R. Tomasello, E. Martinez, R. Zivieri, L. Torres, M. Carpentieri, and G. Finocchio, Sci. Rep. **4**, 6784 (2014).
[7]A. Hirohata, K. Yamada, Y. Nakatani, I.-L. Prejbeanu, B. Dieny, P. Pirro, and B. Hillebrands, J. Magn. Magn. Mater. **509**, 166711 (2020).
[8]X. Zhang, Y. Zhou, K. M. Song, T.-E. Park, J. Xia, M. Ezawa, X. Liu, W. Zhao, G. Zhao, and S. Woo, J. Phys.: Condens. Matter **32**(14), 143001 (2020).
[9]W. J. Jiang, X. C. Zhang, G. Q. Yu, W. Zhang, X. Wang, M. B. Jungfleisch, J. E. Pearson, X. M. Cheng, O. Heinonen, K. L. Wang, Y. Zhou, A. Hoffmann, and S. G. E. te Velthuis, Nat. Phys. **13**(2), 162 (2017).
[10]A. Fert, V. Cros, and J. Sampaio, Nat. Nanotechnol. **8**(3), 152 (2013).
[11]Kazus, vanmsh, njamnKrür, Pdramassran, ucasCara, KornRchr, Fünr, KojSao, O., Rakov, and Johanns Försr, Nat. Phys. **13**(2), 170 (2017).
[12]J. Zang, M. Mostovoy, J. H. Han, and N. Nagaosa, Phys. Rev. Lett. **107**(13), 136804 (2011).
[13]N. Nagaosa and Y. Tokura, Nat. Nanotechnol. **8**(12), 899 (2013).
[14]X. C. Zhang, Y. Zhou, and M. Ezawa, Nat. Commun. **7**, 10293 (2016).
[15]M. Finazzi, M. Savoini, A. R. Khorsand, A. Tsukamoto, A. Itoh, L. Duo, A. Kirilyuk, T. Rasing, and M. Ezawa, Phys. Rev. Lett. **110**(17), 177205 (2013).
[16]J. Hagemeister, A. Siemens, L. Rozsa, E. Y. Vedmedenko, and R. Wiesendanger, Phys. Rev. B **97**(17), 174436 (2018).
[17]N. Mehmood, X. Song, G. Tian, Z. Hou, D. Chen, Z. Fan, M. Qin, X. Gao, and J.-M. Liu, J. Phys. D: Appl. Phys. **53**(1), 014007 (2020).
[18]D. S. Han, S. K. Kim, J. Y. Lee, S. J. Hermsdoerfer, H. Schultheiss, B. Leven, and B. Hillebrands, Appl. Phys. Lett. **94**(11), 112502 (2009).
[19]J. Iwasaki, A. J. Beekman, and N. Nagaosa, Phys. Rev. B **89**(6), 064412 (2014).
[20]X.-G. Wang, G.-H. Guo, Y.-Z. Nie, G.-F. Zhang, and Z.-X. Li, Phys. Rev. B **86**, 054445 (2012).
[21]W. Wang, M. Albert, M. Beg, M.-A. Bisotti, and D. Chernyshenko, Phys. Rev. Lett. **114**(8), 087203 (2015).
[22]J. Xia, Y. Huang, X. Zhang, W. Kang, C. Zheng, X. Liu, W. Zhao, and Y. Zhou, J. Appl. Phys. **122**(15), 153901 (2017).
[23]G. Yin, Y. Liu, Y. Barlas, J. Zang, and R. K. Lake, Phys. Rev. B **92**(2), 024411 (2015).
[24]X. Zhang, M. Ezawa, D. Xiao, G. P. Zhao, and Y. Zhou, Nanotechnology **26**(22), 225701 (2015).
[25]M. K. Shen, Y. Zhang, O. Y. Jun, X. F. Yang, and L. You, Appl. Phys. Lett. **112**(6), 062403 (2018).
[26]S. Li, J. Xia, X. C. Zhang, M. Ezawa, W. Kang, X. X. Liu, Y. Zhou, and W. S. Zhao, Appl. Phys. Lett. **112**(14), 142404 (2018).
[27]S. Rohart and A. Thiaville, Phys. Rev. B **88**(18), 184422 (2013).
[28]S. Zhang and Z. Li, Phys. Rev. Lett. **93**(12), 127204 (2004).
[29]Y. Zhang, S. Luo, X. Yang, and C. Yang, Sci. Rep. **7**, 2047 (2017).
[30]Y. Zhou and M. Ezawa, Nat. Commun. **5**, 4652 (2014).
[31]Y. Zhou, E. Iacocca, A. A. Awad, R. K. Dumas, F. C. Zhang, H. B. Braun, and J. Åkerman, Nat. Commun. **6**, 8193 (2015).
[32]S. Woo, M. Mann, A. J. Tan, L. Caretta, and G. S. D. Beach, Appl. Phys. Lett. **105**(21), 212404 (2014).
[33]P. J. Metaxas, J. P. Jamet, A. Mougin, M. Cormier, J. Ferre, V. Baltz, B. Rodmacq, B. Dieny, and R. L. Stamps, Phys. Rev. Lett. **99**(21), 217208 (2007).
[34]X. Liang, X. C. Zhang, L. C. Shen, J. Xia, M. Ezawa, X. X. Liu, and Y. Zhou, Phys. Rev. B **104**(17), 174421 (2021).
[35]M. Shen, Y. Zhang, L. You, and X. Yang, Appl. Phys. Lett. **113**(15), 152401 (2018).